

Aspects of the Cosmological Electroweak Phase Transition

D. Bödeker^a, W. Buchmüller^b, Z. Fodor^{b*} and T. Helbig^b

a II. Institut für Theoretische Physik, Universität Hamburg, Germany

b Deutsches Elektronen-Synchrotron DESY, Hamburg, Germany

Abstract

We study the decay of the metastable symmetric phase in the standard model at finite temperature. For the SU(2)-Higgs model the two wave function correction terms $Z_\varphi(\varphi^2, T)$ and $Z_\chi(\varphi^2, T)$ of Higgs and Goldstone boson fields are calculated to one-loop order. We find that the derivative expansion of the effective action is reliable for Higgs masses smaller than the W-boson mass. We propose a new procedure to evaluate the decay rate by first integrating out the vector field and the components of the scalar fields with non-zero Matsubara frequencies. The static part of the scalar field is treated in the saddle point approximation. As a by-product we obtain a formula for the decay rate of a homogeneous unstable state. The course of the cosmological electroweak phase transition is evaluated numerically for different Higgs boson masses and non-vanishing magnetic mass of the gauge boson. For Higgs masses above ~ 60 GeV the latent heat can reheat the system to the critical temperature, which qualitatively changes the nature of the transition.

*On leave from Institute for Theoretical Physics, Eötvös University, Budapest, Hungary

1 Introduction

At high temperatures the spontaneously broken symmetry of electroweak interactions is restored [1]-[3]. This is a direct consequence of the Higgs mechanism of symmetry breaking, and the corresponding phase transition is an intriguing aspect of electroweak interactions. It is also of great cosmological importance since at temperatures of order the critical temperature of the phase transition baryon-number violating processes fall out of thermal equilibrium [4]. As a result, the present cosmological baryon asymmetry is finally determined at the electroweak phase transition.

Theoretical descriptions of the phase transition start from the finite-temperature effective potential whose local minima yield the free energy of states with a homogeneous Higgs field given by the position of the local minimum (cf. [5]). Considerable effort has been devoted to evaluate the effective potential in perturbation theory [6]-[10] where, due to infrared divergences, a useful expansion is only obtained after a resummation of an infinite number of terms. Alternatively, interesting first results have been obtained by lattice Monte Carlo simulations [11]-[13], reduced three-dimensional action [14] and by using an average action at finite temperature [15].

The decay of a metastable homogeneous state involves “critical droplets” and therefore inhomogeneous field configurations. The free energy of these configurations is usually estimated based on an effective action which is the sum of the finite-temperature effective potential and the canonical kinetic term of the Higgs field. We will improve this approximation by evaluating the finite-temperature wave function correction terms of the SU(2)-Higgs model to one-loop order. This will allow us to determine the range of Higgs boson masses for which the derivative expansion of the effective action is reliable.

Following Langer’s theory of metastability [16] we evaluate the decay rate in the semiclassical approximation where one starts from some approximate “coarse-grained” effective action and expands around its saddle point interpolating between the symmetric and the broken phase. For finite-temperature quantum field theories the “coarse-grained” effective action is frequently approximated by the one-loop effective potential together with canonical kinetic terms for the scalar fields. The Callan-Coleman theory for the decay of the false vacuum at zero temperature in four dimensions [17] is then applied to the effective three-dimensional theory at finite temperature [18].

One problem, which points to some inconsistency of this approximation, is that the occurring effective potential is in general complex. The origin of this problem in the calculation of the decay rate is the incorrect treatment of the scalar fluctuations which

appear twice, as contribution to the effective potential and as fluctuations around the saddle point. Instead, one has to split the functional integration into two parts, such that the first one yields a “coarse-grained” effective action which has a barrier between the symmetric and the broken phase. In the second part a perturbative expansion is then performed around the non-trivial saddle point, and only here long wave length scalar fluctuations appear. In this spirit, in [19] the integration over the vector fields has been performed in the first step. The same approach has been followed in [20] for the analogous problem of the Coleman-Weinberg model at zero temperature, in citebfhw for nonabelian gauge theories and in [21] for Yukawa models at finite temperature. Here we will further improve these calculations by integrating in the first step also over the components of the scalar fields with non-zero Matsubara frequencies. This will lead us to a “coarse-grained” effective action which is similar to, but not identical with the one used by Dine et al. [6].

Several aspects of the cosmological electroweak phase transition, such as nucleation and growth of critical droplets, wall velocity, transition time etc. have already been discussed in the literature (cf. [6], [9],[22]-[25]). We shall use our results on the finite-temperature effective action to study in more detail the dependence of the course of the phase transition on the Higgs boson mass and also the influence of a non-zero magnetic mass of the W-boson. Our numerical calculations show that reheating effects can qualitatively change the nature of the transition for Higgs masses larger than ~ 60 GeV.

The paper is organized as follows. In sect. 2 we evaluate the two wave function correction factors for the SU(2)-Higgs model to one-loop order. The decay of metastable and unstable homogeneous states is discussed in sect. 3. The course of the phase transition is studied analytically and also in detail numerically in sect. 4. The main results are summarized in sect. 5.

2 The effective action at finite temperature

Consider the SU(2)-Higgs model at finite temperature which is described by the action

$$S_\beta[\Phi, W] = \int_\beta dx \left(-\frac{1}{4} W_{\mu\nu}^a W^{a\mu\nu} + (D_\mu \Phi)^\dagger (D^\mu \Phi) - V_0(\varphi^2) \right) \quad , \quad (1)$$

where

$$V_0(\varphi^2) = \frac{1}{2} \mu^2 \varphi^2 + \frac{1}{4} \lambda \varphi^4 \quad , \quad \frac{1}{2} \varphi^2 \equiv \Phi^\dagger \Phi \quad , \\ \int_\beta dx \equiv \int_0^\beta d\tau \int d^3x \quad , \quad \beta \equiv \frac{1}{T} \quad . \quad (2)$$

D_μ and $W_{\mu\nu}^a$ are the covariant derivative and the Yang-Mills field strength, respectively. The gauge fixing part of the lagrangian has been omitted, and we will always work in Landau gauge. The SU(2)-Higgs model contains the essential features of the standard model of electroweak interactions. Setting $\sin\theta_W = 0$, one neglects the mass difference between Z- and W-boson relative to the W-boson mass. This corresponds to the present accuracy in the description of the electroweak phase transition. We include the effects of the three generations of quarks and leptons with the usual gauge and Yukawa couplings.

In order to find the thermal equilibrium states and to compute properties of the first-order phase transition we have to know the effective action $\Gamma_\beta[\Phi]$ of the theory at finite temperature as functional of the Higgs field Φ which, after gauge fixing, plays the role of an order parameter. The effective action can be expressed as a functional integral

$$e^{-\Gamma_\beta[\Phi]} = \int_\beta [D\hat{\Phi}][D\hat{W}_\mu] \exp\left(-S_\beta[\Phi + \hat{\Phi}, \hat{W}] + \int_\beta dx \frac{\delta\Gamma_\beta[\Phi]}{\delta\Phi(x)} \hat{\Phi}(x)\right) \quad , \quad (3)$$

where the integration extends over fields with periodic boundary conditions in τ . Again, gauge fixing and ghost terms have not been written explicitly. For stationary, τ -independent fields $\Phi(\vec{x})$ the effective action corresponds to the free energy density of the system,

$$\Gamma_\beta[\Phi] = \beta F[\Phi, T] \quad . \quad (4)$$

Ordinary perturbation theory to any finite order does not yield a good approximation to $\Gamma_\beta[\Phi]$ as the scalar masses are negative for small values of φ , and because of the infrared behaviour of the finite-temperature perturbation series.

A systematic expansion in the gauge coupling g and the scalar self-coupling λ is obtained by means of a resummation, where in all propagators the tree-level masses are replaced by one-loop plasma masses to order g^2 and λ (cf. [9]). The mass differences are then treated as counter terms,

$$\delta S_\beta = -\frac{1}{2} \int_\beta dx \left[W^{a\mu} \left(\delta m_L^2 P_{L\mu\nu} + \delta m_T^2 P_{T\mu\nu} \right) W^{a\nu} - \delta m_\varphi^2 \varphi^2 - \delta m_\chi^2 \chi^2 \right] \quad . \quad (5)$$

Here P_L and P_T are the usual projection operators on longitudinal and transverse degrees of freedom of the vector field (cf. [5]). The plasma mass terms δm_i^2 are the differences between the masses

$$m_L^2 = \frac{11}{6} g^2 T^2 + \frac{g^2 \varphi^2}{4} \quad , \quad (6)$$

$$m_T^2 = \frac{g^2 \varphi^2}{4} \quad , \quad (7)$$

$$m_\varphi^2 = \left(\frac{3}{16}g^2 + \frac{\lambda}{2} + \frac{1}{4}f_t^2 \right) (T^2 - T_b^2) + 3\lambda\varphi^2 \quad , \quad (8)$$

$$m_\chi^2 = \left(\frac{3}{16}g^2 + \frac{\lambda}{2} + \frac{1}{4}f_t^2 \right) (T^2 - T_b^2) + \lambda\varphi^2 \quad , \quad (9)$$

and the tree-level masses

$$m^2 = \frac{1}{4}g^2\varphi^2 \quad , \quad \bar{m}_\varphi^2 = \lambda(3\varphi^2 - v^2) \quad , \quad \bar{m}_\chi^2 = \lambda(\varphi^2 - v^2) \quad . \quad (10)$$

In the plasma masses we have included the effect of the top-quark loop, with $m_t = f_tv/\sqrt{2}$. The temperature T_b , at which the barrier between the symmetric and the broken phase vanishes, reads in leading order of the couplings

$$T_b^2 = \frac{16\lambda v^2}{3g^2 + 8\lambda + 4f_t^2} \quad . \quad (11)$$

Note, that the tree-level Higgs- and Goldstone-boson masses are obtained from the scalar potential by ($\varphi^2 = \sum_{I=1}^4 \varphi_I \varphi_I$)

$$\frac{\partial^2 V_0}{\partial \varphi_I \partial \varphi_J} = \bar{m}_\varphi^2 P_{IJ}^\varphi + \bar{m}_\chi^2 P_{IJ}^\chi \quad , \quad (12)$$

where

$$P_{IJ}^\varphi = \frac{\varphi_I \varphi_J}{\varphi^2} \quad , \quad P_{IJ}^\chi = \delta_{IJ} - \frac{\varphi_I \varphi_J}{\varphi^2} \quad (13)$$

are the projection operators on the Higgs and the Goldstone fields.

At one-loop order the improved perturbation theory yields the effective potential to order g^3 , $\lambda^{3/2}$,

$$\begin{aligned} V_{eff}(\varphi^2, T) &= \frac{1}{2} \left(\frac{3g^2}{16} + \frac{\lambda}{2} + \frac{1}{4}f_t^2 \right) (T^2 - T_b^2)\varphi^2 + \frac{\lambda}{4}\varphi^4 \\ &\quad - (3m_L^3 + 6m_T^3 + m_\varphi^3 + 3m_\chi^3) \frac{T}{12\pi} + \mathcal{O}(g^4, \lambda^2, f_t^4), \end{aligned} \quad (14)$$

which is equivalent to the result of the ring summation [7]. Several two-loop contributions are also known. For the SU(2)-Higgs model the effective potential has been calculated to order g^4 , λ [8], and for the abelian Higgs model it is known to order e^4 , λ^2 [26].

The strength of the electroweak phase transition is rather sensitive to the magnetic mass of the gauge bosons, whose calculation requires non-perturbative techniques. In Landau gauge the one-loop gap equations yield $m_T = (g^2/3\pi)T$ at $\varphi = 0$ [9],[10]. In order to estimate its effect on parameters of the phase transition we will replace eq. (7) by

$$m_T^2 = \gamma^2 \frac{g^4}{9\pi^2} T^2 + \frac{g^2}{4} \varphi^2 \quad , \quad (15)$$

and compute sensitive quantities for different values of γ .

The effective potential (14) has degenerate local minima at $\varphi = 0$ and $\varphi = \varphi_c > 0$ at a critical temperature T_c and therefore predicts a first-order phase transition. The evaluation of the transition rate requires knowledge of a stationary point of the free energy which interpolates between the two local minima. The effective action (3) can be expanded in powers of derivatives, and for time-independent fields one has

$$\Gamma_\beta[\Phi] = \beta \int d^3x \left(V_{eff}(\varphi^2, T) + \frac{1}{2}(\delta_{IJ} + Z_{IJ}(\Phi, T))\vec{\nabla}\varphi_I\vec{\nabla}\varphi_J + \dots \right) \quad . \quad (16)$$

From eqs. (3) and (16) it is obvious that the functions Z_{IJ} can be obtained from the inverse scalar propagator in the homogeneous scalar background field Φ with spacial momentum \vec{k} ,

$$\begin{aligned} D^{-1}(\vec{k}^2, \Phi, T)_{IJ} &= \vec{k}^2\delta_{IJ} + \frac{\partial^2 V_0(\varphi^2)}{\partial\varphi_I\partial\varphi_J} + i\Sigma_{IJ}(\vec{k}^2, \Phi, T) \\ &= m_\varphi^2(\varphi^2, T)P_{IJ}^\varphi + m_\chi^2(\varphi^2, T)P_{IJ}^\chi \\ &\quad + (\delta_{IJ} + Z_{IJ}(\Phi, T))\vec{k}^2 + \mathcal{O}(\|\vec{\Delta}\|) \quad . \end{aligned} \quad (17)$$

The one-loop contributions to Z_{IJ} are shown in fig. (1). It is a well-known problem in finite temperature field theory that the order of a given Feynman graph can be smaller than the order coming from the vertices. This is due to the fact that loop diagrams accumulate couplings in the denominators which decrease the power of the usual couplings coming from the Feynman rules. In appendix A we show that only graphs of the type shown in fig. 1 give contributions to the wave function correction in leading order, where one has to include not only the tree level but also the plasma masses for internal lines. Note, that the knowledge of the effective action for static fields is not sufficient if one is interested in time-dependent processes such as the thermalization of perturbations [27].

Eq. (16) is an expansion in powers of $(\vec{\nabla}/m_i)^2$, where m_i denotes all masses which appear in propagators of internal lines. Clearly, the terms with zero Matsubara frequencies for the internal lines dominate, since they have the smallest denominators. For the same reason the top-quark contribution is suppressed, since all Matsubara frequencies are non-zero for fermions. It is straightforward to evaluate the contributions of fig. (1) as function of the couplings g and λ , the scalar propagators

$$\Delta(\vec{k}^2, m_i^2) = \frac{1}{\vec{k}^2 + m_i^2} \quad , \quad (18)$$

and the vector propagator

$$D_{\mu\nu}(\vec{k}) = \Delta(\vec{k}^2, m_L^2)P_{L\mu\nu} + \Delta(\vec{k}^2, m_T^2)P_{T\mu\nu} \quad . \quad (19)$$

After some algebra one obtains a sum of integrals of the type

$$I(\vec{k}^2, m_1^2, m_2^2) = T \int \frac{d^3l}{(2\pi)^3} \Delta(\vec{l}^2, m_1^2) \Delta((\vec{l} + \vec{k})^2, m_2^2) \quad (20)$$

$$= \frac{T}{4\pi |\vec{k}|} \arctan \frac{|\vec{k}|}{m_1 + m_2} \quad (21)$$

$$= \frac{1}{4\pi} \frac{T}{m_1 + m_2} \left(1 - \frac{1}{3} \frac{\vec{k}^2}{(m_1 + m_2)^2} + \mathcal{O}(\|\vec{\Delta}\|) \right) . \quad (22)$$

Collecting all terms we obtain the final result

$$Z_{IJ}(\Phi, T) = Z_\varphi(\varphi^2, T) P_{IJ}^\varphi + Z_\chi(\varphi^2, T) P_{IJ}^\chi , \quad (23)$$

where

$$Z_\varphi(\varphi^2, T) = \frac{T}{4\pi} \left[\frac{1}{4} \lambda \bar{m}^2 \left(\frac{3}{m_\varphi^3} + \frac{1}{m_\chi^3} \right) - 2g^2 \frac{1}{m_\chi + m_T} + \frac{1}{8} g^2 m^2 \left(\frac{1}{2m_L^3} + \frac{5}{m_T^3} \right) \right] \quad (24)$$

and

$$Z_\chi(\varphi^2, T) = \frac{T}{6\pi} \left[\frac{2\lambda \bar{m}^2}{(m_\varphi + m_\chi)^3} - g^2 \left(\frac{2}{m_\chi + m_T} + \frac{1}{m_\varphi + m_T} \right) \right] , \quad (25)$$

with $\bar{m}^2 = \lambda\varphi^2$ and $m^2 = g^2\varphi^2/4$. In terms of the complex field Φ this result can be written as

$$\frac{1}{2} Z_{IJ} \vec{\nabla}_I \varphi_I \vec{\nabla}_J \varphi_J = \frac{1}{4} (\Phi^\dagger \Phi)^{-1} [\vec{\nabla}(\Phi^\dagger \Phi)]^2 Z_\varphi + \left(\vec{\nabla} \Phi^\dagger \vec{\nabla} \Phi - \frac{1}{4} (\Phi^\dagger \Phi)^{-1} [\vec{\nabla}(\Phi^\dagger \Phi)]^2 \right) Z_\chi . \quad (26)$$

(For completeness we give in appendix A the wave function correction term $Z(\varphi^2, T)$ for the abelian Higgs model.) The Z -factor Z_φ for the Higgs field is dominated by the contribution from the transverse vector boson loop which, if one neglects the magnetic mass, diverges at $\varphi \sim 0$,

$$Z_\varphi(\varphi^2, T) \sim \frac{5g^2 T}{16\pi \varphi} . \quad (27)$$

Neglecting plasma mass terms for the vector bosons and using $m_L = m_T \gg m_\chi$ one obtains instead

$$Z_\varphi(\varphi^2, T) \sim -\frac{21g^2 T}{32\pi \varphi} . \quad (28)$$

This agrees with the result of a previous calculation by Moss et al. [28] who used a different technique. The comparison of eqs. (27) and (28) shows the important difference between the ordinary and the improved perturbation theory with plasma masses¹. The

¹In a very recent paper [29] Z_φ has also been calculated using the improved perturbation theory. Our results differ from those obtained by these authors. The differences can be traced back to the treatment of the mass counter terms of eq. (5).

order of magnitude for Z_φ is the same in both cases, the sign, however, has changed. Wave function correction terms in the 't Hooft-Feynman background gauge have recently been evaluated in [30]. Note, that despite the divergence of Z_φ at $\varphi \sim 0$ the correction to the surface tension $\sigma = \int_0^{\varphi_c} d\varphi \sqrt{2(1 + Z_\varphi(\varphi^2, T_c))V_{eff}(\varphi^2, T_c)}$ is finite.

What is the effect of the wave function factors $Z(\varphi^2, T)$ on parameters describing the electroweak phase transition? The first-order phase transition is due to the barrier in the effective potential (14) which is essentially generated by the vector-boson loops. This implies that at the critical temperature T_c the magnitude of the local minimum in the broken phase is $\varphi_c/T_c \sim g^3/\lambda$. One also easily verifies that $(T_c^2 - T_b^2)/T_c^2 \sim g^4/\lambda$. Hence, in the effective potential (14) the terms quadratic, cubic and quartic in φ are all of order $\sim (g^{12}/\lambda^3)T_c^4$. The perturbative approach is only reliable if this energy density is larger than the density due to the magnetic mass of the W-boson, which is of order $m_T^3 T_c \sim g^6 T_c^4$. Hence a necessary condition for the smallness of non-perturbative effects is $\lambda < g^2$. Further, if one uses the high-temperature expansion one has to satisfy $g\varphi_c/T_c < 1$, i.e., $\lambda > g^4$. In this case the allowed range of λ is given by $g^4 < \lambda < g^2$.

A naive estimate of the size of $Z(\varphi_c^2, T_c)$ can now be obtained based on eqs. (6) - (9), (24) and (25). One easily verifies that, at φ_c and T_c , the plasma masses are of order

$$m_T \sim \frac{g^4}{\lambda} T_c < m_L \quad , \quad m_{\varphi, \chi} \sim \frac{g^3}{\sqrt{\lambda}} T_c \quad . \quad (29)$$

From eqs. (24), (25) one then concludes

$$Z_{\varphi, \chi} = \mathcal{O}\left(\frac{\lambda}{\lambda \epsilon}\right) \quad . \quad (30)$$

Hence, for the allowed range of couplings determined from the effective potential corrections due to the Z -factors can be treated as perturbation.

Clearly, these estimates are rather naive. As the saddle point of the effective action, which interpolates between the two local minima, varies from $\varphi = 0$ to $\varphi = \varphi_c$, the full scalar mass terms

$$m_\varphi^2 = \frac{\partial^2 V_{eff}(\varphi^2, T)}{\partial \varphi^2}, \quad m_\chi^2 = \frac{1}{\varphi} \frac{\partial V_{eff}(\varphi^2, T)}{\partial \varphi} \quad (31)$$

become negative and the expansion in powers of derivatives breaks down. Even for positive mass terms this expansion is problematic for stationary points of the effective action. For these field configurations

$$\begin{aligned} \vec{\nabla}^2 \varphi &= \frac{\partial}{\partial \varphi} V_{eff}(\varphi^2, T) \\ &= m_\chi^2 \varphi. \end{aligned} \quad (32)$$

the equation of motion shows that $\vec{\nabla}/m_i = \mathcal{O}(1)$. Hence, higher order terms in the derivative expansion are non-negligible. As we shall see in the following section, a more careful treatment nevertheless confirms the above conclusion on the size of the wave function correction terms.

3 Decay of the false vacuum

At temperatures below the critical temperature T_c the symmetric phase becomes metastable and decays via nucleation and growth of droplets of the broken phase. In condensed matter physics a theory for the decay of such metastable states has been developed by Langer many years ago [16]. Starting from the Fokker-Planck equation for the probability distribution of droplets with different sizes, Langer derived an expression for the nucleation rate in terms of a saddle-point $\bar{\varphi}$ of the free energy which interpolates between the two phases. A similar result for the decay rate has been obtained by applying the Callan-Coleman theory for the decay of the false vacuum at zero temperature in four dimensions [17] to the effective three-dimensional theory at finite temperature [18]. We will base our discussion on Langer's theory according to which the decay rate is given by

$$\Gamma = \frac{\kappa}{2\pi} \frac{\text{Im}Z_\beta[\bar{\Phi}]}{Z_\beta[\Phi = 0]} \quad , \quad Z_\beta[\Phi] = e^{-\Gamma_\beta[\Phi]} \quad , \quad (33)$$

where Γ_β is given by eq. (3). The "dynamical factor" κ has recently been evaluated in terms of viscosities of the electroweak plasma [25]. The rate (33) is determined using a time independent solution of the Fokker-Planck equation. This is justified because the characteristic time scales of the microscopic processes (e.g., WW scattering) are several orders of magnitude smaller than the time needed for the phase transition. Thus, the Langer theory is applicable, and it is sufficient to use a stationary solution of the Fokker-Planck equation.

The non-trivial phase structure of the Higgs models at finite temperature becomes only apparent if quantum fluctuations are taken into account. The tree-level potential possesses only a single local minimum at $\varphi \neq 0$. This is analogous to the case of Coleman-Weinberg symmetry breaking by radiative corrections. In order to obtain the decay rate one first has to integrate out degrees of freedom which generate the barrier between the symmetric and the broken phase and only then, in a second step, determine the interpolating saddle point. In [19] it has been suggested to first integrate out the vector field. The same route has been followed in the abelian Higgs model at zero temperature

and Coleman-Weinberg symmetry breaking [20]. This method has then been extended to the standard model [9] and Yukawa models [21].

Here we suggest to improve this method in the following way. In eq. (33) the background field Φ depends only on spatial coordinates. Therefore in the classical action S_β , which appears in the integrand of the functional integral, only the quantum field $\hat{\Phi}_0$ is shifted, i.e., the mode with zero Matsubara frequency,

$$\hat{\Phi}(\tau, \vec{x}) = \sum_n \hat{\Phi}_n(\vec{x}) e^{i\omega_n \tau} \quad , \quad \omega_n = 2\pi n T \quad . \quad (34)$$

This suggests to integrate out the scalar fields with non-zero Matsubara frequencies in addition to the vector fields. Since the "Compton-wave lengths" of these modes are smaller than the wall thickness of the critical droplet, this procedure should yield an appropriate effective action which plays the role of the "coarse-grained" free energy in Langer's calculation. The scalar part of the functional integral is therefore split,

$$D\hat{\Phi} = \prod_n D\hat{\Phi}_n = D\hat{\Phi}_0 \prod_{n \neq 0} D\hat{\Phi}_n \quad , \quad (35)$$

and in the first step all modes except $\hat{\Phi}_0$ are integrated out.

The functional integral over vector fields and the non-zero frequency modes of the scalar field yields an effective action $\tilde{\Gamma}_\beta$ which replaces the classical action S_β in eq. (33),

$$\begin{aligned} e^{-\Gamma_\beta[\Phi]} &= \int_\beta [D\hat{\Phi}_0] \prod_{n \neq 0} \int [D\hat{\Phi}_n] \int_\beta [DW] \exp \left(-S_\beta[\Phi + \hat{\Phi}, W] + \int d^3x \frac{\delta \Gamma_\beta[\Phi]}{\delta \Phi(\vec{x})} \hat{\Phi}(\vec{x}) \right) \\ &= \int_\beta [D\hat{\Phi}_0] \exp \left(-\tilde{\Gamma}_\beta[\Phi + \hat{\Phi}_0] + \int d^3x \frac{\delta \Gamma_\beta[\Phi]}{\delta \Phi(\vec{x})} \hat{\Phi}_0(\vec{x}) \right) \quad . \end{aligned} \quad (36)$$

At one-loop order one obtains for the effective action $\tilde{\Gamma}_\beta$ a sum of terms of the type calculated in sect. 2, where now the zero-frequency contribution of the scalar fields are absent in the loop integrals. In addition there is a non-local contribution which stems from the integration over the vector field,

$$\begin{aligned} \tilde{\Gamma}_\beta[\Phi] &= \tilde{\Gamma}_\beta^{(1)}[\Phi] + \tilde{\Gamma}_\beta^{(2)}[\Phi] \quad , \\ \tilde{\Gamma}_\beta^{(1)}[\Phi] &= \beta \int d^3x \left(\tilde{V}_{eff}(\varphi^2, T) + \frac{1}{2} (\delta_{IJ} + \tilde{Z}_{IJ}(\varphi^2, T)) \vec{\nabla} \varphi_I \vec{\nabla} \varphi_J + \dots \right) \quad , \\ \tilde{\Gamma}_\beta^{(2)}[\Phi] &= \frac{g^2}{2} \beta \int d^3x d^3x' J_\mu^a(\vec{x}) D_T^{\mu\nu}(\vec{x}, \vec{x}') J_\nu^a(\vec{x}') \quad , \end{aligned} \quad (37)$$

where $J_\mu^a = \frac{1}{2} (\Phi^\dagger \partial_\mu \tau^a \Phi - \partial_\mu \Phi^\dagger \tau^a \Phi)$ is the SU(2)-current and $D_{T\mu\nu}$ is the propagator for the transverse part of the vector field in the background field $\Phi(\vec{x})$.

The difference between the effective potentials is given by

$$\begin{aligned} \frac{\partial}{\partial\varphi} (V_{eff} - \tilde{V}_{eff}) &= -3T\lambda\varphi \int \frac{d^3k}{(2\pi)^3} \left(\frac{1}{\vec{k}^2 + m_\varphi^2} + \frac{1}{\vec{k}^2 + m_\chi^2} \right) \\ &= \frac{3\lambda}{4\pi} \varphi T (m_\varphi + m_\chi + C) \quad . \end{aligned} \quad (38)$$

Here C is a linearly divergent constant which vanishes in dimensional regularization. We have explicitly checked that for other regularizations it cancels against the sum of divergent terms which arise from integration over fields with non-zero Matsubara frequencies. To leading order in the couplings the masses m_φ and m_χ are given by eqs. (8) and (9). Integrating eq. (38) gives precisely the cubic scalar terms in the potential (14). Hence, defining the split (34) of the functional integral in dimensional regularization one obtains to order $\mathcal{O}(\lambda^3, \lambda^{\geq 4/\epsilon})$

$$\begin{aligned} \tilde{V}_{eff}(\varphi^2, T) &= \frac{1}{2} \left(\frac{3g^2}{16} + \frac{\lambda}{2} + \frac{1}{4}f_t^2 \right) (T^2 - T_b^2)\varphi^2 + \frac{\lambda}{4}\varphi^4 \\ &\quad - (3m_L^3 + 6m_T^3) \frac{T}{12\pi} + \mathcal{O}(g^4, \lambda^2)T_b^4 \quad , \end{aligned} \quad (39)$$

where

$$\begin{aligned} m_L^2 &= \frac{11}{6}g^2T^2 + \frac{g^2\varphi^2}{4} \quad , \\ m_T^2 &= \gamma^2 \frac{g^4}{9\pi^2}T^2 + \frac{g^2}{4}\varphi^2 \quad . \end{aligned}$$

The effective potential \tilde{V}_{eff} is similar to the potential used by Dine et al. [6] to describe the electroweak phase transition. For $\varphi \ll T$ the term linear in T essentially becomes the one-loop vector boson contribution reduced by a factor 1/3 [6]. To estimate the size of non-perturbative corrections we have kept a non-zero magnetic mass with an order of magnitude given by the one-loop gap equations [9],[10]. A novel feature of the potential (39) is the way in which contributions from scalar loops are treated. There are no terms cubic in the scalar masses, since the integration over $\hat{\Phi}_0$ has not been carried out. However, contrary to the treatment in [6], the scalar-loop contributions to the term quadratic in φ are kept, since they arise from integration over $\hat{\Phi}_n$, $n \neq 0$. This has an important effect on the difference between critical temperature and barrier temperature of the transition. For $m_H = 60$ GeV we find an increase by a factor of two.

We conclude that keeping the contribution of scalar loops to the T^2 -term in the effective potential and dropping the cubic scalar mass terms yields the correct effective potential for the zero-Matsubara frequency part of the scalar field.

As discussed in sect. 2, the part of the Z -factors arises from the zero-frequency contributions to the loop integrals. Hence, pure vector boson loops give the dominant contribution to \tilde{Z} , since the integration over $\hat{\Phi}_0$ is not carried out. The result is easily read off from eqs. (24),(25),

$$\begin{aligned}\tilde{Z}_\varphi(\varphi^2, T) &= \frac{T}{32\pi} g^2 m^2 \left(\frac{1}{2m_L^3} + \frac{5}{m_T^3} \right) \quad , \\ \tilde{Z}_\chi(\varphi^2, T) &= 0 \quad .\end{aligned}\tag{40}$$

The "coarse-grained" effective action $\tilde{\Gamma}_\beta$ is now given by eqs. (37),(39) and (40). Note, \tilde{Z}_φ is positive. Hence, the surface tension and therefore the strength of the phase transition is increased. \tilde{Z}_φ is shown in fig. (2) for three different values of the magnetic mass.

Using eqs. (33) - (40) we can now calculate the decay rate of the metastable symmetric phase. As discussed in sect. 2, the Z -factors $Z_{\varphi,\chi}$ are expected to yield only small corrections. Therefore we start from $Z = 0$ and the effective potential (39) and determine a saddle point $\bar{\varphi}$ which interpolates between the symmetric and the broken phase. The remaining $\hat{\Phi}_0$ -integration is then carried out in the Gaussian approximation. The spectrum of fluctuations contains one negative eigenvalue λ_- which guarantees that $Z_\beta[\bar{\varphi}]$ is purely imaginary. Further, there are six zero modes from translational invariance and global $SU(2)\times U(1)$ symmetry, and a discrete and continuous positive spectrum. The contribution of the zero-modes to the fluctuation determinant is given by [9]

$$\begin{aligned}\mathcal{V}_{trans} V &= \left(\frac{1}{2\pi} \tilde{\Gamma}_\beta[\bar{\Phi}] \right)^{3/2} V, \\ \mathcal{V}_{int} &= \frac{\pi^2}{2} \left(\frac{\beta}{2\pi} \int d^3x \bar{\varphi}^2 \right)^{3/2},\end{aligned}\tag{41}$$

where V is the total volume of the physical three-dimensional space. In the thin wall approximation also the contribution from "Goldstone modes" has been evaluated [9], which correspond to deformations of the droplet surface. However, for the electroweak phase transition the thin wall approximation is known not to be reliable [6],[25]. We therefore base our calculations on the decay rate (cf. (33), (41))

$$\frac{\Gamma}{V} = \kappa |\lambda_-|^{-1/2} \mathcal{V}_{\perp\nabla\rightarrow\lambda} \mathcal{V}_{\lambda\perp} \mu' \mathcal{I}^{-\heartsuit}_\beta[\mathcal{A}] = \mathcal{A} \mathcal{I}^{-\heartsuit}_\beta[\mathcal{A}] \quad ,\tag{42}$$

where $\bar{\varphi}$ is the saddle point and $\mu = m_\varphi(0, T)$. The negative eigenvalue λ_- is approximated by $-2/R^2$, its thin wall value, where the radius R of the critical droplet is defined by $\partial^2 \bar{\varphi}(r = R, T)/\partial r^2 = 0$. κ can be estimated using the results given in [25].

We have numerically determined the saddle point $\bar{\varphi}$ at temperatures close to the critical temperature T_c for different values of the scalar self-coupling λ and the parameter γ ,

i.e., the magnetic mass m_T . This will be described in more detail in the following section. Fig. (3) shows the ratio of the pre-factor in eq. (42) normalized to T^4 as function of the Higgs mass at the respective temperature T_e where the phase transition is completed. Clearly, the logarithm of the pre-factor is much smaller than $\Gamma_\beta[\bar{\varphi}]$ which, at the temperature T_e , is ~ 140 . Hence, the semiclassical approximation is justified. The difference between the pre-factor A and T^4 is numerically unimportant for the description of the cosmological phase transition. As the Higgs mass m_H approaches the critical mass m_H^{crit} , where the transition becomes second-order for $\gamma \neq 0$, the pre-factor strongly decreases. This is mostly due to the decrease of μ .

A measure for the size of the one-loop correction to the Z -factor is the ratio

$$\delta_Z = \frac{\int d^3x \tilde{Z}_{\bar{\varphi}} (\vec{\nabla} \bar{\varphi})^2}{\int d^3x (\vec{\nabla} \bar{\varphi})^2} . \quad (43)$$

This correction is shown in fig. (4) as function of the Higgs mass for different values of γ . For $\gamma = 0$ the perturbative expansion breaks down at $m_H \sim 80$ GeV, in agreement with results obtained previously [9]. For $\gamma = 1, 2$ the correction never exceeds 10% which demonstrates the importance of the infrared cutoff provided by the magnetic mass.

The effective potential to order $\mathcal{O}(\lambda^\exists, \lambda^{\exists/\epsilon})$ is given by eq. (14). The corresponding quantity without the one-loop contribution of the static part of the scalar field Φ is \tilde{V}_{eff} (39). A more accurate approximation to the effective potential can be obtained by performing the $\hat{\Phi}_0$ -integration over the expression (36) in the Gaussian approximation. The result is the potential

$$\bar{V}_{eff} = \tilde{V}_{eff} - \frac{T}{12\pi} (m_\varphi^3 + 3m_\chi^3) , \quad (44)$$

where, contrary to eq. (14), the scalar masses are now given by

$$m_\varphi^2 = \frac{\partial^2 \tilde{V}_{eff}(\varphi^2)}{\partial \varphi^2} , \quad m_\chi^2 = \frac{1}{\varphi} \frac{\partial \tilde{V}_{eff}(\varphi^2)}{\partial \varphi} . \quad (45)$$

These masses agree with the mass terms (8) and (9) only to leading order in the couplings. The potentials V_{eff} and \bar{V}_{eff} clearly differ by an infinite number of terms, if the masses (45) are formally expanded in powers of λ . The most important property of the mass terms (45) is that they become negative as the scalar field varies between the two local minima of \tilde{V}_{eff} . Hence, the true effective potential \bar{V} is complex. This general feature of non-convex potentials, which is well known for models at zero temperature, is not visible to any finite order in perturbation theory.

What is the meaning of the imaginary part of the effective potential? At zero temperature the imaginary part is defined by first substituting

$$m^2(\varphi) \rightarrow m^2(\varphi) - i\epsilon \quad , \quad (46)$$

and then performing the limit $\epsilon \rightarrow 0$. This yields the imaginary part

$$\mathcal{I}(\varphi) = 2 \operatorname{Im}V(\varphi) \quad (47)$$

$$= \frac{1}{32\pi} |m^2(\varphi)|^2 \Theta(-m^2(\varphi)) \quad (48)$$

which is interpreted as decay rate per unit time and volume of the homogeneous state into inhomogeneous states of lower energy [31].

It is straightforward to adopt the same procedure at finite temperature. One immediately obtains from the cubic scalar mass terms in eq. (44)

$$\mathcal{I}_\beta(\varphi) = 2 \operatorname{Im}\bar{V}_{eff}(\varphi, T) \quad (49)$$

$$= \frac{T}{6\pi} (|m_\varphi^2|^{3/2} \Theta(-m_\varphi^2) + |m_\chi^2|^{3/2} \Theta(-m_\chi^2)) \quad . \quad (50)$$

This should then be the finite-temperature decay width of a homogeneous state into mixed states. This interpretation appears sensible at a stationary point φ of the potential $\bar{V}(\varphi^2, T)$ where $m_\chi = 0$, i.e., eq. (49) should be applicable at the top of the barrier. For arbitrary values of φ the interpretation of the rate (49) is less clear due to the gauge dependence of this expression.

4 The cosmological phase transition

We can now use the results obtained in the last section to investigate the cosmological electroweak phase transition. This phase transition has already been studied in considerable detail by several groups [6],[9],[22]-[25]. Here we will extend the previous studies mainly in two respects. We shall study the dependence of the transition on the mass of the Higgs boson, and we shall also investigate the influence of a non-zero magnetic mass. In this case the transition becomes second order for Higgs masses above a critical mass m_H^{crit} [9], and the reheating of the symmetric phase can qualitatively change the nature of the transition.

The main features of the transition can be understood by considering the simplified potential

$$V = \frac{1}{2}a(T^2 - T_b^2)\varphi^2 - \frac{1}{3}bT\varphi^3 + \frac{1}{4}\lambda\varphi^4 \quad , \quad (51)$$

where the parameters a and b can be read off from eq. (39). Here we neglect m_L , which contributes essentially only to the T^4 -term, and set $\gamma = 0$. An analytical treatment of the transition is possible in the thin wall approximation [18]. Quantitatively, this approximation is too crude for the electroweak phase transition. However, it is still useful to get a qualitative picture of the transition and to obtain the order of magnitude of the various parameters involved. This will be confirmed by our numerical calculations discussed below.

In the thin wall approximation the nucleation rate is given by

$$\frac{\Gamma(t)}{V} = A \exp\left(-B \left(\frac{t_c}{t_c - t}\right)^2\right) , \quad (52)$$

where

$$A = \omega T_b^4 \quad , \quad B = \frac{\sqrt{2} 2^6 \pi b^5}{3^{20} a^2 \lambda^{7/2}} \quad , \quad (53)$$

with $\omega = \mathcal{O}(\infty)$. T_b is the barrier temperature, and t_c is the time at which the critical temperature $T_c \approx T_b$ is reached. Using eqs. (11), (39) and the relation between time and temperature, $t \approx 0.03 m_{PL}/T^2$ with $m_{PL} = 1.2 \cdot 10^{19}$ GeV [32], one obtains the relations

$$T_b = 120 \text{ GeV } G_F^{-1/2} (3m_W^2 + m_H^2 + 2m_t^2)^{-1/2} \left(\frac{m_H}{100\text{GeV}}\right) \quad , \quad (54)$$

$$t_c = 1.7 \cdot 10^{-11} \text{ sec } G_F (3m_W^2 + m_H^2 + 2m_t^2) \left(\frac{100\text{GeV}}{m_H}\right)^2 \quad , \quad (55)$$

$$B = \frac{2^{10}}{3^4 \pi^4} \frac{G_F^2 m_W^{15}}{(3m_W^2 + m_H^2 + 2m_t^2)^2 m_H^7} \quad . \quad (56)$$

$$(57)$$

From these equations one can read off the involved orders of magnitude of time and temperature and also the dependence on the Higgs boson mass.

As the universe expands the temperature T decreases. Once the critical temperature T_c is reached critical droplets can start to nucleate and grow. At time t the number density of droplets of size r is

$$n(t, r) = \Gamma \left(t - \frac{r}{v}\right) \quad . \quad (58)$$

Here v is the velocity of the droplet wall, and the initial size of the critical droplet has been neglected. The fraction of space filled with the new phase is then

$$f_B(t) = \exp\left(-\frac{4\pi}{3} \int_0^{r_{max}(t)} dr r^3 n(t, r)\right) \quad , \quad r_{max}(t) = v(t - t_c) \quad , \quad (59)$$

where the exponentiation in eq. (59) accounts for the overlap between different droplets.

The phase transition is completed at time t_e , which one may define implicitly by $f_B(t_e) = 1/e$. The nucleation rate is non-negligible only for times very close to t_e . This allows one to derive simple expressions for the time t_e , the “transition time” τ during which the phase transition essentially takes place, the total number of droplets $N(t)$ per unit volume and the average radius $\bar{R}(t)$, which are defined as

$$N(t) = \int_0^{r_{max}(t)} dr n(t, r) \quad , \quad (60)$$

$$\bar{R}(t) = \frac{1}{N(t)} \int_0^{r_{max}(t)} dr r n(t, r) \quad . \quad (61)$$

A straightforward calculation yields for the time t_e the implicit relation

$$\frac{\pi A t_c^4}{2 B^4} \left(\frac{t_e - t_c}{t_c} \right)^{12} \exp \left(-B \left(\frac{t_c}{t_e - t_c} \right)^2 \right) = 1 \quad , \quad (62)$$

and for the transition time τ one obtains

$$\tau = \frac{(t_e - t_c)^3}{2Bt_c^2} \quad . \quad (63)$$

The fraction of converted space, the number of droplets and the average radius are given by

$$f_B(t) \approx \exp \left(-\exp \left(\frac{t_e - t}{\tau} \right) \right) \quad , \quad (64)$$

$$N(t) \approx \frac{1}{8\pi\tau^3} \exp \left(\frac{t_e - t}{\tau} \right) \quad , \quad (65)$$

$$\bar{R}(t) \approx \tau \quad . \quad (66)$$

These equations demonstrate that the phase transition takes place in the time interval τ before t_e . Using eqs. (55),(56), (62) and (63) one easily verifies the following hierarchy between the different time scales

$$t_c \gg t_e - t_c \gg \tau \quad . \quad (67)$$

We have also studied the phase transition numerically. Here the free energy of the critical droplet is calculated using the potential \tilde{V}_{eff} (cf. (39)) derived in sect. 3. We keep a non-zero magnetic mass of the size given by the one-loop gap equations, i.e., we choose $\gamma = 1$ in eq. (15). For the potential (39) the stationary point $\bar{\varphi}$ and the corresponding free energy are determined numerically for temperatures below T_c down to T_e , where the transition is completed. The course of the transition depends on the velocity of the

droplet wall which has been discussed in detail in the literature [6],[23],[24]. Here we just illustrate the dependence by calculating the course of the transition for three different velocities, $v = c$, $v = c/10$ and $v = c/1000$. The initial radius of the critical droplet, which is very small (cf. [9]), is also taken into account.

Figs. (5) - (8) show the result for $m_H = 30$ GeV, which we have chosen as an example of a small Higgs mass. The completion time t_e is $\sim 3 \cdot 10^{-12}$ sec and depends only weakly on the wall velocity (fig. (5)). As one may have expected, the number of droplets (fig. (6)) and the average radius (fig. (7)) at the end of the transition scale approximately like v^{-3} and v^{-1} . The number density of droplets is given per cm^3 . Note, that the size of the horizon at the critical temperature is of order 1 cm. Following Enqvist et al. [22] and Carrington and Kapusta [25] we have plotted in fig. (8) the change in temperature as function of time. The system supercools from time t_c until the time t_s at which the supercooling stops and the liberated latent heat leads to some reheating. The increase in temperature can be estimated by

$$\Delta T_R = \frac{1}{c_v} L \quad , \quad (68)$$

where the latent heat is given by the derivative of the effective potential,

$$L = T \left. \frac{\partial}{\partial T} \tilde{V}_{eff}(T, \varphi^2) \right|_{T=T_c} \quad , \quad (69)$$

and the specific heat of the symmetric phase is

$$c_v = \frac{d}{dT} e(T) \quad , \quad e(T) = \frac{427}{120} \pi^2 T^4 \quad . \quad (70)$$

Here $e(T)$ is the energy density of the standard model at high temperatures to leading order in the coupling constants, where gluons and the U(1)-gauge boson have been included. The above equations are easily derived from the usual thermodynamic relations and the relations for the pressure $p_s(T) = -\tilde{V}_{eff}(T, 0)$ and $p_b(T) = -\tilde{V}_{eff}(T, \varphi^2(T))$ in the symmetric and broken phase, respectively. Using these equations to compute the reheating temperature assumes that the wall velocity is sufficiently small so that the latent heat can indeed be converted into thermal energy of the symmetric phase.

In fig. (8) the true evolution is compared with a transition where thermal equilibrium is maintained at all times. In this hypothetical case the temperature remains at T_c until the time t'_e , at which all latent heat has been used up to expand the universe. At later times the cooling due to the expansion then proceeds in the usual manner. Note that the real phase transition starts after considerable supercooling and completes in a very

short time. The temperature after reheating is slightly larger than the temperature of the adiabatic transition at the same time. This is due to the entropy generated in the transition.

For the Higgs mass $m_H = 60$ GeV the transition looks qualitatively the same. The time interval $t_s - t_c$ decreases by about two orders of magnitude to $\sim 2 \cdot 10^{-14}$ sec (fig. (9)). Correspondingly, the average radius decreases by about two orders of magnitude whereas the number density of droplets increases by about six orders. Since much less time is available for supercooling, the temperature after reheating is now closer to the critical temperature T_c than for $m_H = 30$ GeV. Our numerical results for $m_H = 60$ GeV are consistent with those obtained in [25], given the differences in the choice of m_t , the magnetic mass and the wall velocity.

A dramatic change occurs for $m_H = 80$ GeV (fig. (10)). After the initial supercooling period the liberated latent heat starts to reheat the system at the time $t_s < t'_e$, long before the transition is completed. Due to the small supercooling the latent heat can reheat the system to the critical temperature. After that no new droplets nucleate, the average radius \bar{R} increases linear with time, and the transition completes in equilibrium (fig. (10)), resembling the QCD phase transition [22]. Compared to $m_H = 60$ GeV the time interval $t_s - t_c$ has decreased again by two orders of magnitude to $\sim 3 \cdot 10^{-16}$ sec. Contrary to the QCD phase transition the time difference $t'_e - t_c$ is much smaller than the Hubble time due to the smallness of the latent heat.

The change of the nature of the phase transition for large values of the Higgs mass is a consequence of the magnetic mass. For any finite value of this mass, the phase transition becomes very weakly first-order with rising Higgs mass and eventually second-order above a critical Higgs mass m_H^{crit} [9]. Our calculations show that below this critical value there is a large range of Higgs masses for which the universe reheats up to T_c . This is shown in fig. (11) where the reheating temperature ΔT_R is compared with the supercooling temperature needed to initiate the phase transition ΔT_{SC} . Clearly, the reheating temperature reaches T_c if $\Delta T_R > \Delta T_{SC}$.

This interesting result can also be understood analytically. Consider a potential with a generic plasma mass, in our case the simplified potential (51) with non-zero magnetic mass,

$$V = \frac{1}{2}a(T^2 - T_b^2)\varphi^2 - \frac{1}{3}bT(c^2T^2 + \varphi^2)^{3/2} + \frac{1}{4}\lambda\varphi^4 \quad . \quad (71)$$

This potential implies a change from a first-order to a second-order phase transition as the Higgs mass increases. Since there are strong hints that the magnetic mass is non-

zero, we expect that eq. (71) is a reasonable approximation for the effective potential of the standard model. Above a critical value of the scalar coupling,

$$\lambda_{crit} = \frac{b}{2c} \quad , \quad (72)$$

the potential (71) describes a second-order phase transition. For values of λ slightly below λ_{crit} the transition is weakly first-order. We are interested in the behaviour of several quantities as λ approaches λ_{crit} from below. The position φ_c of the degenerate minimum at T_c vanishes in this limit. Some other characteristic quantities of the first-order transition vanish as powers of φ_c . We find for the mass difference Δm , the maximum of the effective potential V^{max} , the surface tension σ , the transition rate Γ , the latent heat L and the temperature differences $T_c - T_b$ and $T_c - T_s$, where T_s is the temperature corresponding to t_s ,

$$\begin{aligned} \Delta m \equiv m_H^{crit} - m_H &\sim \varphi_c^2 \quad , \\ V^{max} &\sim \varphi_c^6 \quad , \\ \sigma &\sim \varphi_c^4 \quad , \\ L &\sim \varphi_c^2 \quad , \\ \Gamma &\sim \varphi_c^0 \quad , \\ T_c - T_b &\sim \varphi_c^2 \quad , \\ T_c - T_s &\sim \varphi_c^4 \quad . \end{aligned} \quad (73)$$

Using these equations one obtains for t_s , the time at which the supercooling stops for the true transition, and for t'_e , the time for which the equilibrium transitions complete, respectively,

$$\begin{aligned} t_s - t_c &\sim T_c - T_s \sim \varphi_c^4 \sim \Delta m^2 \quad , \\ t'_e - t_c &\sim L \sim \varphi_c^2 \sim \Delta m \quad . \end{aligned} \quad (74)$$

Clearly, for Higgs masses very close to m_H^{crit} one has $t_s < t'_e$, i.e., the supercooling ends, the liberation of the latent heat reheats the system to T_c and the phase transition completes in equilibrium. For vanishing magnetic mass this phenomenon does not occur for Higgs masses smaller than the vector boson mass, for which the perturbative approach is reliable.

5 Summary

In this paper we have extended previous studies of the electroweak phase transition in several respects. In particular, we have studied in greater detail the decay rate for the metastable symmetric phase and also the course of the phase transition. On the whole the by now familiar picture is confirmed that the phase transition is weakly first-order for Higgs boson masses up to the W -boson mass where the perturbative approach becomes unreliable.

We have calculated the two wave function correction factors Z_φ and Z_χ for the $SU(2)$ -Higgs model, and we have evaluated the corresponding correction to the free energy of critical droplets. We find that the perturbative expansion is reliable for Higgs masses below 80 GeV.

The evaluation of the decay rate of the metastable symmetric phase is a non-trivial problem, especially since the metastability is entirely due to quantum corrections. Hence, two expansions are needed, first an improved perturbative expansion to obtain the “coarse-grained” effective action with a barrier between the two local minima, and second the expansion around the critical droplet, the saddle point of the “coarse-grained” effective action. We have improved previous calculations by integrating out the vector fields and the components of the scalar fields with non-zero Matsubara frequencies in the first step. However, further work is still needed to obtain a better understanding of renormalization, gauge dependence and convergence of the performed expansions.

As a by-product of our calculation we have derived a formula for the decay rate of a homogeneous unstable state, which is the finite-temperature analogue of the familiar zero-temperature decay rate. Both formulae are obtained from the imaginary part of the effective potential. The interpretation of the formula away from a local maximum of the potential, in particular its gauge dependence, requires further study.

Our numerical analysis of the course of the cosmological electroweak phase transition shows that at a Higgs boson mass of ~ 60 GeV a qualitative change of the nature of the transition occurs. This is a consequence of the very weak first-order phase transition which in our case is due to the assumed non-zero magnetic mass of the W -boson. For Higgs masses above 60 GeV the reheating temperature reaches the critical temperature before the transition is completed. The phase transition then continues in equilibrium, similar to the QCD phase transition. This may have interesting implications for the generated density fluctuations.

As the Higgs mass increases the phase transition becomes more and more dependent on non-perturbative properties of the symmetric phase. In our calculations this is reflected in the strong dependence on the value of the magnetic mass of the vector boson. Recent lattice calculations indicate that such non-perturbative effects may increase the strength of the first-order transition. A deeper understanding of these non-perturbative effects appears to be a crucial step on the way towards a theory of the electroweak phase transition.

The work of D. B. has been supported by the “Graduiertenkolleg für theoretische Elementarteilchenphysik”, Universität Hamburg. Z. F. acknowledges partial support from Hung. Sci. Grant under Contract No. OTKA-F1041.

Appendix A Contributions to $Z(\Phi, T)$

As it was promised we show that only graphs of the type shown in fig. 1 with plasma mass insertions on the internal lines give contributions in leading order to $Z(\Phi, T)$.

Instead of g , $\sqrt{\lambda}$ and f_t we use in this appendix a generic coupling h .

A diagram can contribute to an order in h lower than the power in h obtained from vertices, if some of the Matsubara frequencies of the loop variables vanish. In the following we call these loops and the corresponding lines soft. Consider a contribution to the effective potential from a graph G of the following type:

- a. it has at least one internal scalar line l_{scalar} ;
- b. by cutting l_{scalar} the diagram remains one-particle irreducible;
- c. r loop variables (among them the momentum of l_{scalar}) are soft;
- d. the loops of non-zero Matsubara frequencies (in the following hard loops) yield leading order plasma mass corrections (cf. fig. 12, where thick lines are hard, thin ones are soft, $r = 2$).

According to appendix A of [9] this graph gives a contribution V_G to the effective potential of order h^{r+2} . Writing V_G as a Feynman integral over \vec{p} (the momentum of l_{scalar}) with the appropriate self-energy insertion $\Sigma_G(p_0 = 0, \vec{p}^2)$ and performing a Taylor-expansion in \vec{p}^2 one gets

$$\begin{aligned}
 V_G &= \int \frac{d^3p}{(2\pi)^3} \frac{1}{\vec{p}^2 + m^2} \Sigma_G(p_0 = 0, \vec{p}^2) \\
 &= \int \frac{d^3p}{(2\pi)^3} \frac{1}{\vec{p}^2 + m^2} \left[\Sigma_G(p_0 = 0, \vec{p}^2 = 0) + \vec{p}^2 \Sigma'_G(p_0 = 0, \vec{p}^2 = 0) + \dots \right] \\
 &= C + h^3 \int \frac{d^3x}{(2\pi)^3} \frac{1}{\vec{x}^2 + 1} \vec{x}^2 \Sigma'_G(p_0 = 0, \vec{p}^2 = 0), \tag{A.1}
 \end{aligned}$$

where $\Sigma'_G = \partial \Sigma_G / \partial \vec{p}^2$, and we have used the substitution $\vec{p} = m\vec{x}$ (remember that m is of order h). Since V_G is of order h^{r+2} and the above integral over \vec{x} is independent of h , the derivative term $\Sigma'(p_0 = 0, \vec{p}^2 = 0)$ is of order h^{r-1} . In our case one-soft-loop contributions with plasma mass corrections to $\Sigma(p_0 = 0, \vec{p}^2)$ correspond to two-soft-loop ($r = 2$) contributions to V_G , thus the wave function correction term is at least of order $h^{2-1} = h$. Summing all plasma mass corrections yields the full propagators of the improved perturbation theory for internal lines. This $\mathcal{O}(\langle \rangle)$ contribution is non-zero and it is given by eqs. (24),(25).

According to (A.16) of [9] other diagrams (eg., diagrams with more soft loops or more complicated hard loop structures then mentioned above) lead to higher order corrections to $Z(\Phi, T)$.

For completeness we also list the Z -factors for a model with n complex fields $\Phi = (\Phi^{(1)}, \dots, \Phi^{(n)})$, $\Phi^{(\alpha)} = (\varphi_1^{(\alpha)} + i\varphi_2^{(\alpha)})\sqrt{2}$, where the diagonal global $U(1)$ symmetry is gauged. At one loop order, zero-Matsubara frequency internal lines yield the wave function correction terms (cf. fig. 1. a,b):

$$\begin{aligned} & \frac{1}{2}Z_{IJ}^{(\alpha\beta)}(\Phi, T)\vec{\nabla}\varphi_I^{(\alpha)}\vec{\nabla}\varphi_J^{(\beta)} = \\ & - \frac{1}{4}(\Phi^\dagger\Phi)^{-1}(\vec{\nabla}\Phi^\dagger\Phi - \Phi^\dagger\vec{\nabla}\Phi)^2 Z_1 + \vec{\nabla}\Phi^\dagger\vec{\nabla}\Phi Z_2 + \frac{1}{4}(\Phi^\dagger\Phi)^{-1}(\vec{\nabla}(\Phi^\dagger\Phi))^2 Z_3, \end{aligned} \quad (\text{A.2})$$

where

$$\begin{aligned} Z_1(\varphi^2, T) &= \frac{2e^2T}{3\pi} \left(\frac{1}{m_\varphi + m_T} - \frac{1}{m_\chi + m_T} \right) \\ Z_2(\varphi^2, T) &= -\frac{2e^2T}{3\pi} \frac{1}{m_\chi + m_T} \\ Z_3(\varphi^2, T) &= \frac{e^2Tm^2}{48\pi} \left(\frac{1}{m_L^3} + \frac{10}{m_T^3} \right), \end{aligned} \quad (\text{A.3})$$

e is the gauge coupling and $m = e\varphi$. For $n = 1$, the usual abelian Higgs model, only two linear combinations contribute, $Z_\chi = Z_2 - Z_1$ and $Z_\varphi = Z_2 + Z_3$.

References

- [1] D. A. Kirzhnits and A. D. Linde, Phys. Lett. B72 (1972) 471
- [2] S. Weinberg, Phys. Rev. D9 (1974) 3357;
L. Dolan and R. Jackiw, Phys. Rev. D9 (1974) 3320
- [3] D. A. Kirzhnits and A. D. Linde, Ann. Phys. 101 (1976) 195
- [4] V. A. Kuzmin, V. A. Rubakov and M. E. Shaposhnikov, Phys. Lett. B155 (1985) 36
- [5] J. I. Kapusta, Finite Temperature Field Theory (Cambridge University Press, Cambridge, 1989)
- [6] M. Dine et al., Phys. Rev. D46 (1992) 550
- [7] M. E. Carrington, Phys. Rev. D45 (1992) 2933
- [8] P. Arnold and O. Espinosa, Phys. Rev. D47 (1993) 3546
- [9] W. Buchmüller, Z. Fodor, T. Helbig and D. Walliser, preprint DESY 93-21
- [10] J.R. Espinosa, M. Quirós and F. Zwirner, Phys. Lett. B314 (1993) 206
- [11] H. G. Evertz, J. Jersák and K. Kanaya, Nucl. Phys. B285 [FS19] (1987) 229
- [12] B. Bunk, E.-M. Ilgenfritz, J. Kripfganz and A. Schiller, Phys. Lett. B284 (1992) 371; Nucl. Phys. B403 (1993) 453
- [13] K. Kajantie, K. Rummukainen and M. Shaposhnikov, preprint CERN-TH 6901/93 (1993)
- [14] H. Meyer-Ortmanns and A. Patkós, Phys. Lett. B297 (1993) 331;
A. Jakovác and A. Patkós, Z. Phys. C60 (1993) 361
- [15] M. Reuter and C. Wetterich, Nucl. Phys. B408 (1993) 91;
N. Tetradis and C. Wetterich, preprint DESY 93-128 (1993)
- [16] J. Langer, Ann. Phys. 41 (1967) 108; *ibid.* 54 (1969) 258
- [17] C. Callan and S. Coleman, Phys. Rev. D16 (1977) 1762
- [18] A. D. Linde, Nucl. Phys. B216 (1983) 421

- [19] W. Buchmüller, T. Helbig and D. Walliser, Nucl. Phys. B407 (1993) 387
- [20] E. J. Weinberg, Phys. Rev. D47 (1993) 4614
- [21] M. Gleiser, G. C. Marques and R. O. Ramos, Phys. Rev. D48 (1993) 2838
- [22] K. Enqvist, J. Ignatius, K. Kajantie and K. Rummukainen, Phys. Rev. D45 (1992) 3415
- [23] N. Turok, Phys. Rev. Lett. 68 (1992) 1803
- [24] B. H. Liu, L. McLerran and N. Turok, Phys. Rev. D46 (1992) 2668
- [25] M. E. Carrington and J. I. Kapusta, Phys. Rev. D47 (1993) 5304
- [26] A. Hebecker, Z. Phys. C60 (1993) 271
- [27] P. Elmfors, K. Enqvist and I. Vilja, preprints NORDITA-93/22 P,-93/48 P (1993)
- [28] I. Moss, D. Toms and A. Wright, Phys. Rev. D46 (1992) 1671
- [29] D.-U. Jungnickel and D. Walliser, preprint FERMI-PUB-93/253-T (1993)
- [30] M. Hellmund, J. Kripfganz and M. G. Schmidt, preprint HD-THEP-93-23 (1993)
- [31] E. J. Weinberg and A. Wu, Phys. Rev. D36 (1987) 2474
- [32] E. W. Kolb and M. Turner, The Early Universe (Addison-Wesley, New York, 1990)

Figure captions

Figure 1: One-loop contributions to the wave function correction factors.

Figure 2: The wave function correction factor \tilde{Z}_φ for three different values of the magnetic mass.

Figure 3: The pre-factor of the decay rate as function of the Higgs boson mass.

Figure 4: One-loop wave function correction as function of the Higgs boson mass m_H for different values of γ .

Figure 5: Volume fraction of the new phase as function of $t - t_c$; $m_H = 30$ GeV.

Figure 6: Number density of droplets per cm^3 as function of $t - t_c$; $m_H = 30$ GeV.

Figure 7: Average droplet radius as function of $t - t_c$; $m_H = 30$ GeV.

Figure 8: Change in temperature of the true (solid line) and the equilibrium (dashed line) transitions as function of $t - t_c$; $m_H = 30$ GeV.

Figure 9: Change in temperature of the true (solid line) and the equilibrium (dashed line) transitions as function of $t - t_c$; $m_H = 60$ GeV.

Figure 10: Change in temperature of the true (solid line) and the equilibrium (dashed line) transitions as function of $t - t_c$; $m_H = 80$ GeV.

Figure 11: Comparison of the temperature decrease due to supercooling and the temperature increase due to reheating as function of the Higgs boson mass.

Figure 12: A two-soft-loop contribution to the effective potential.

Figure 1.

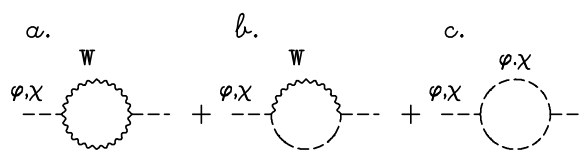


Figure 2.

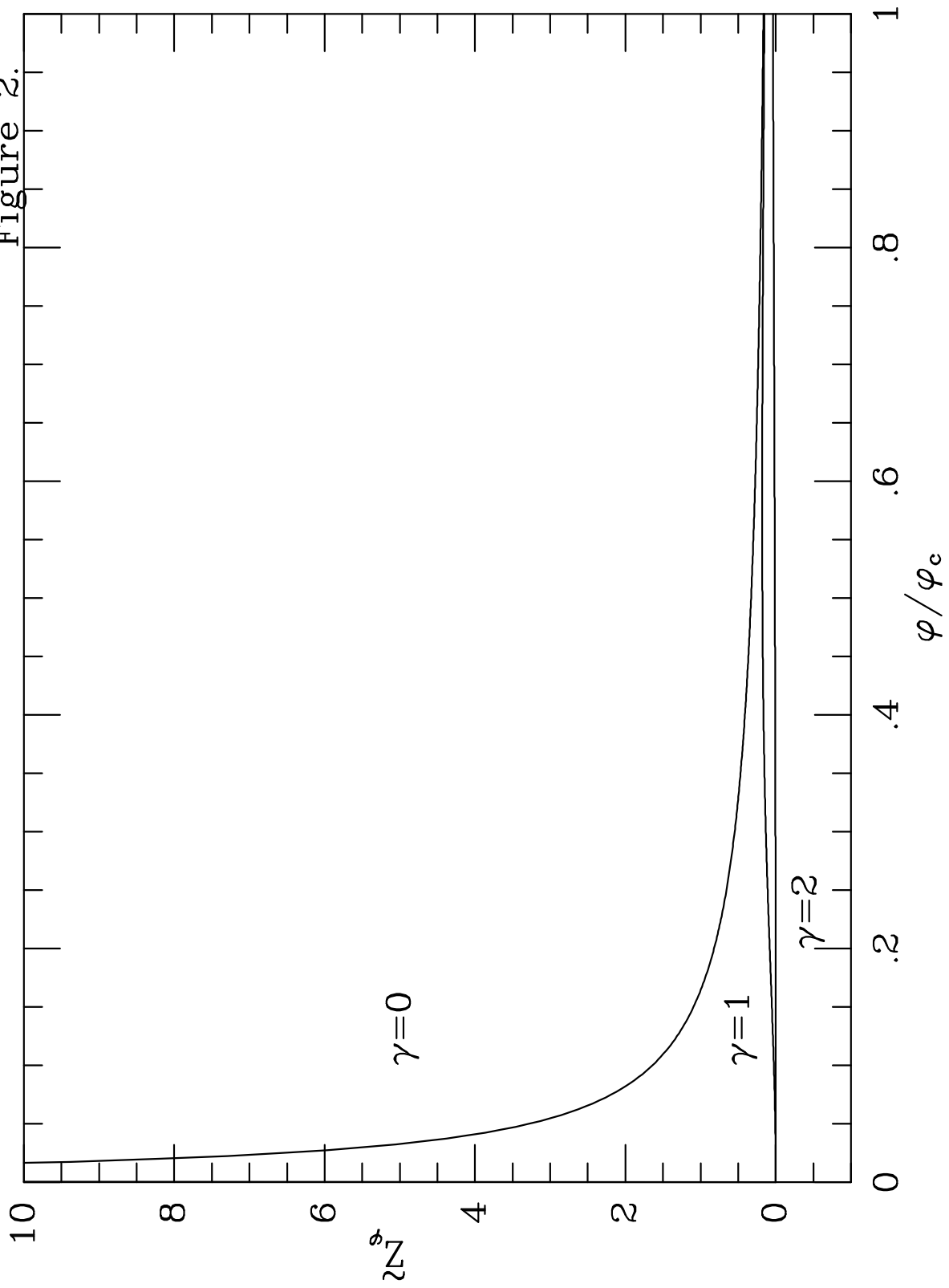


Figure 3.

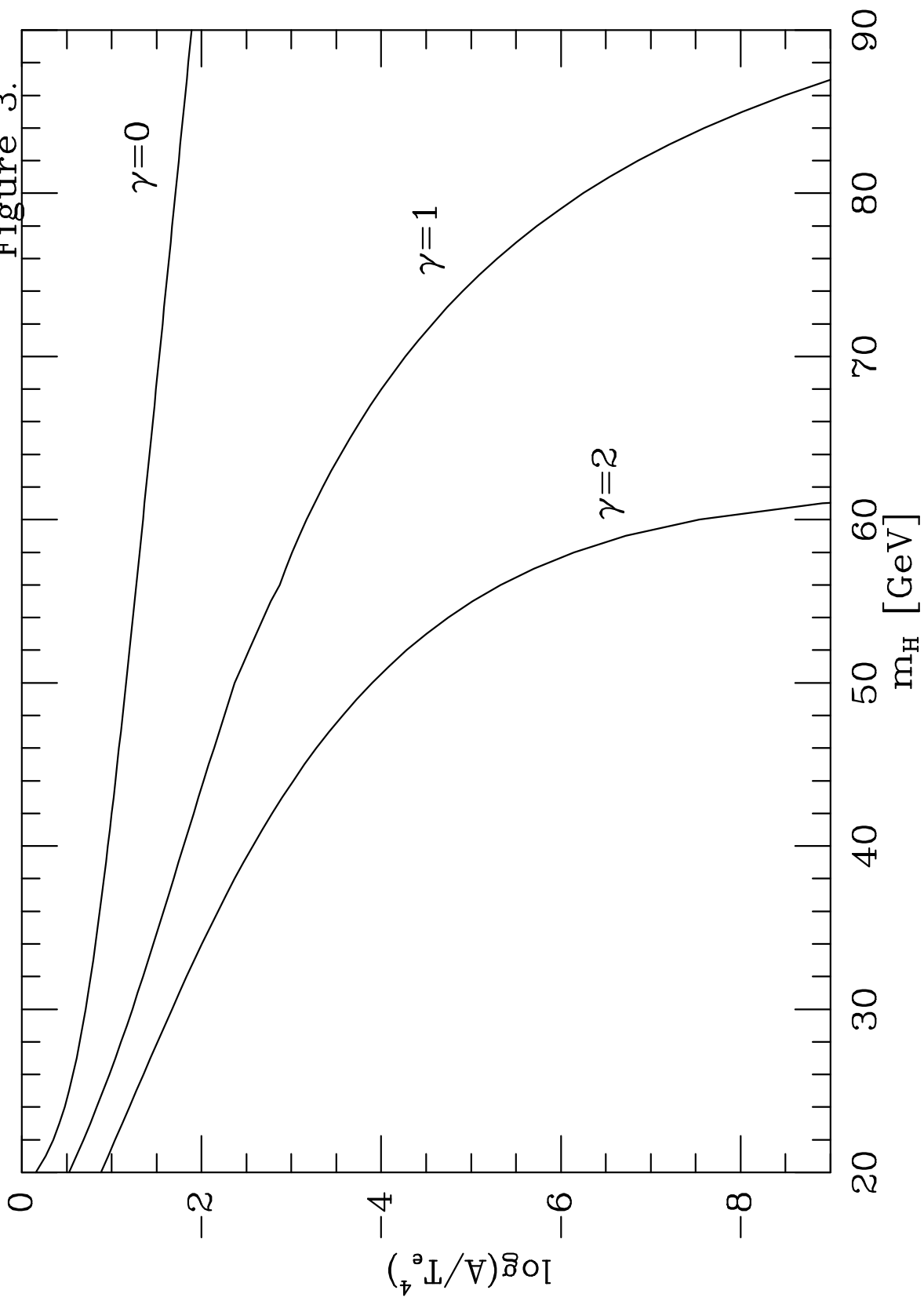


Figure 4.

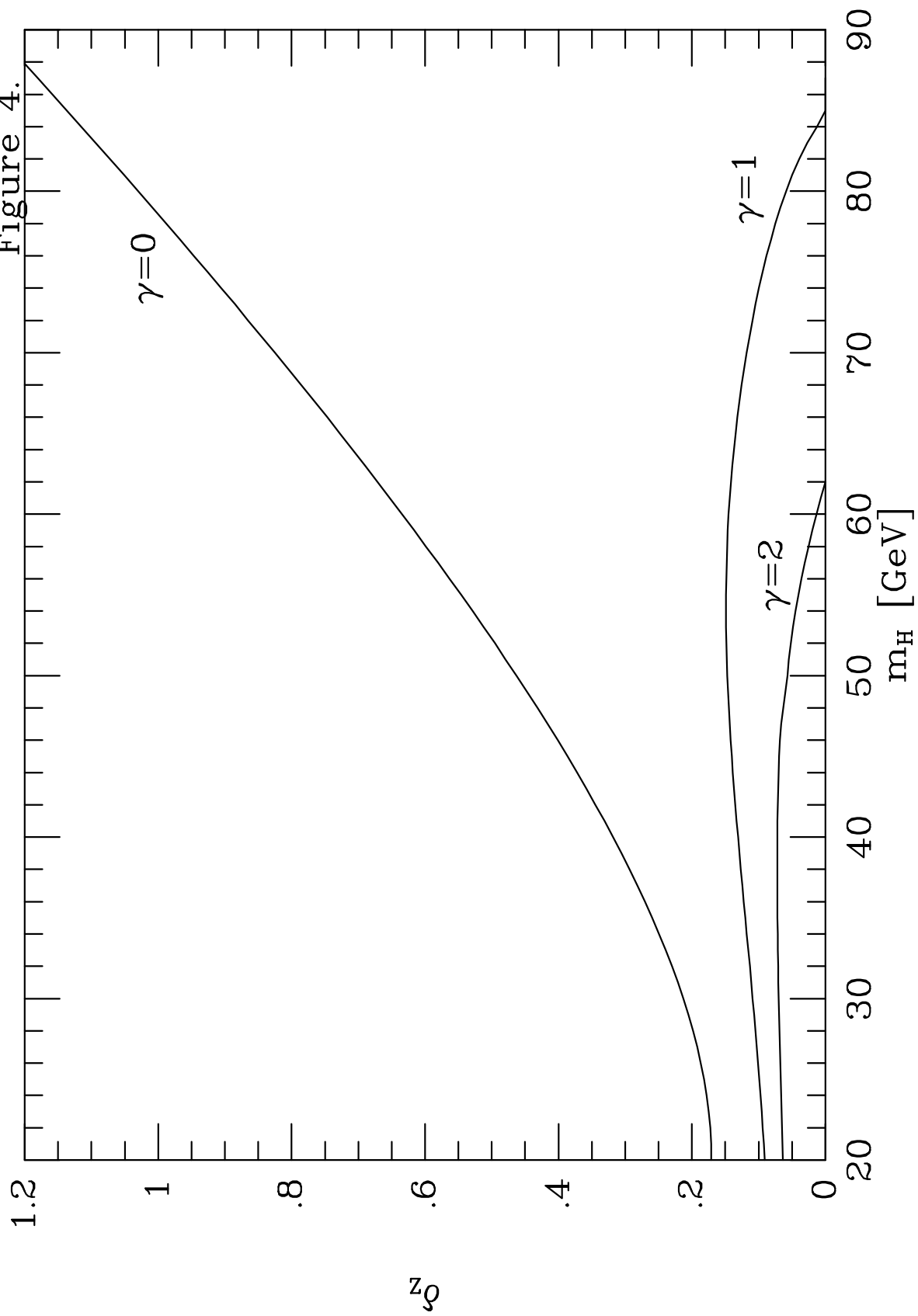


Figure 5.

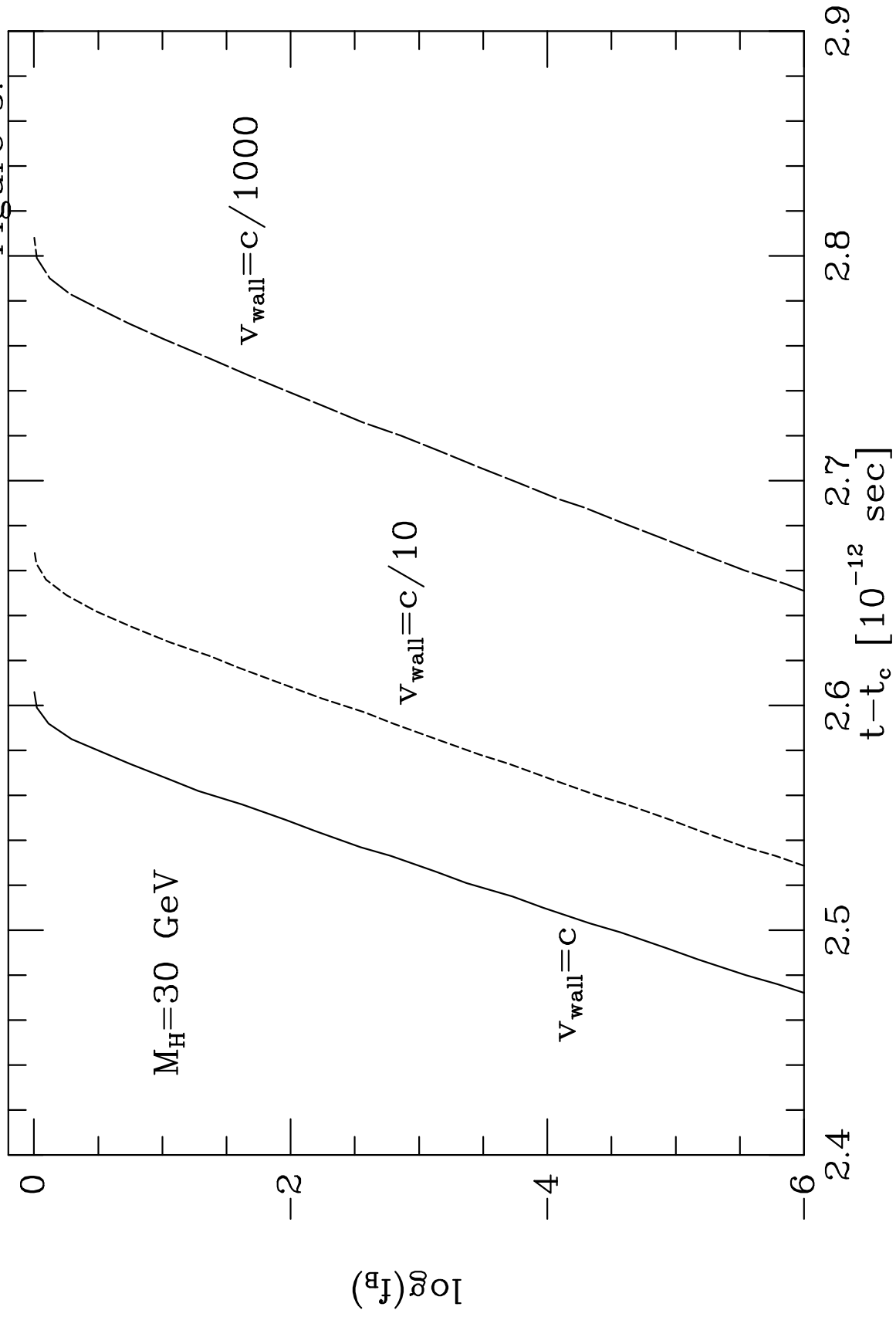


Figure 6.

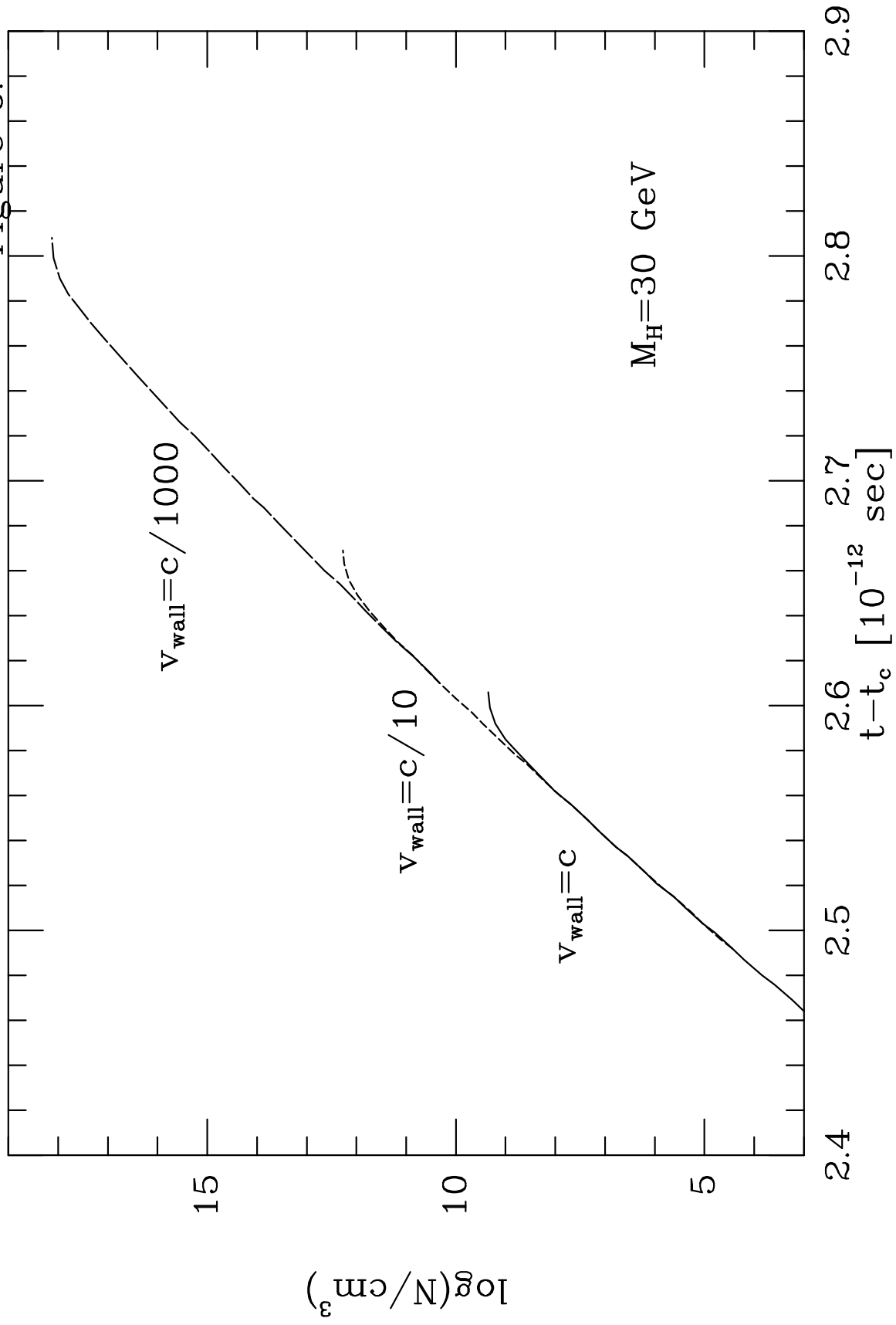


Figure 7.

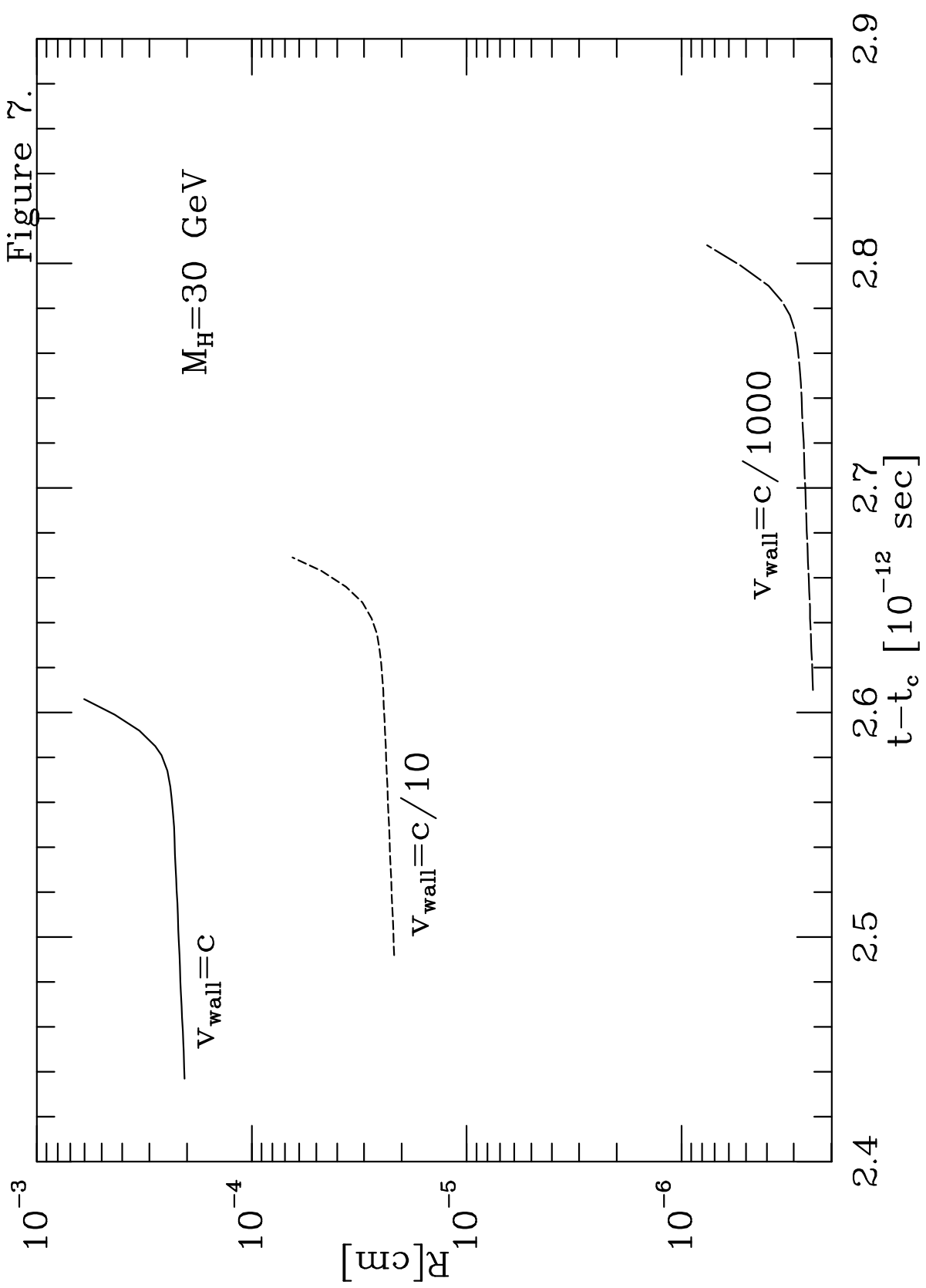


Figure 8.

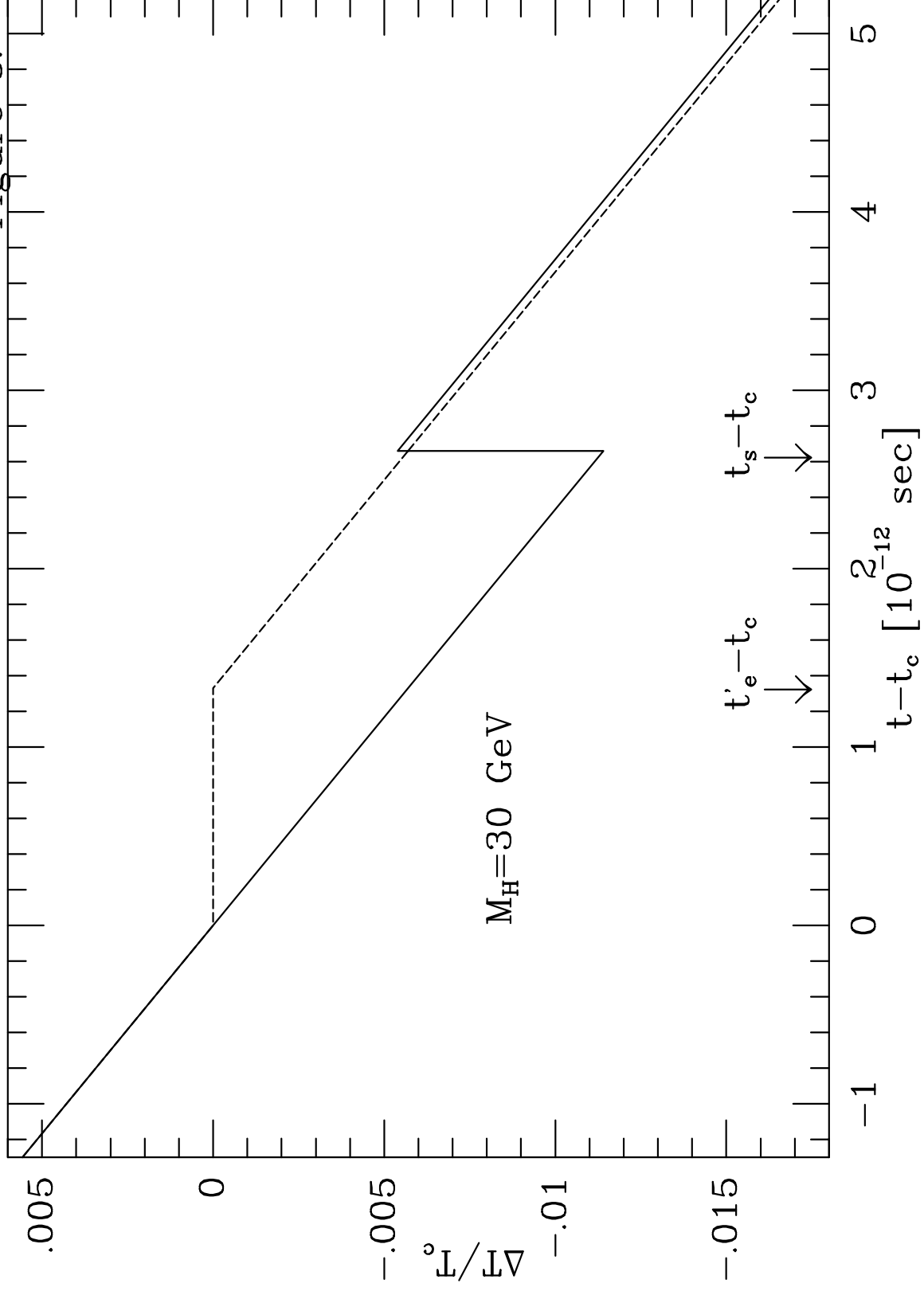


Figure 9.

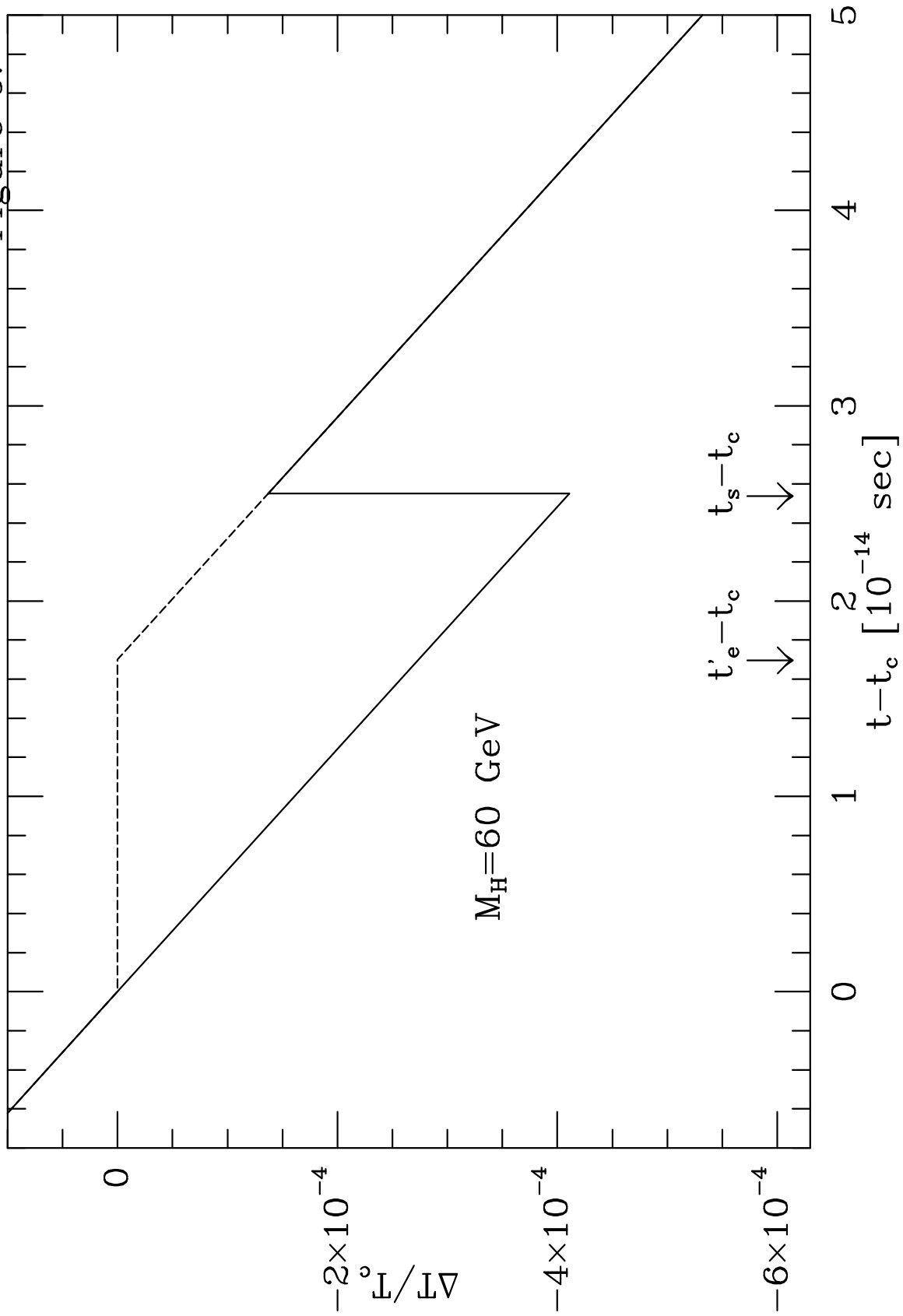


Figure 10.

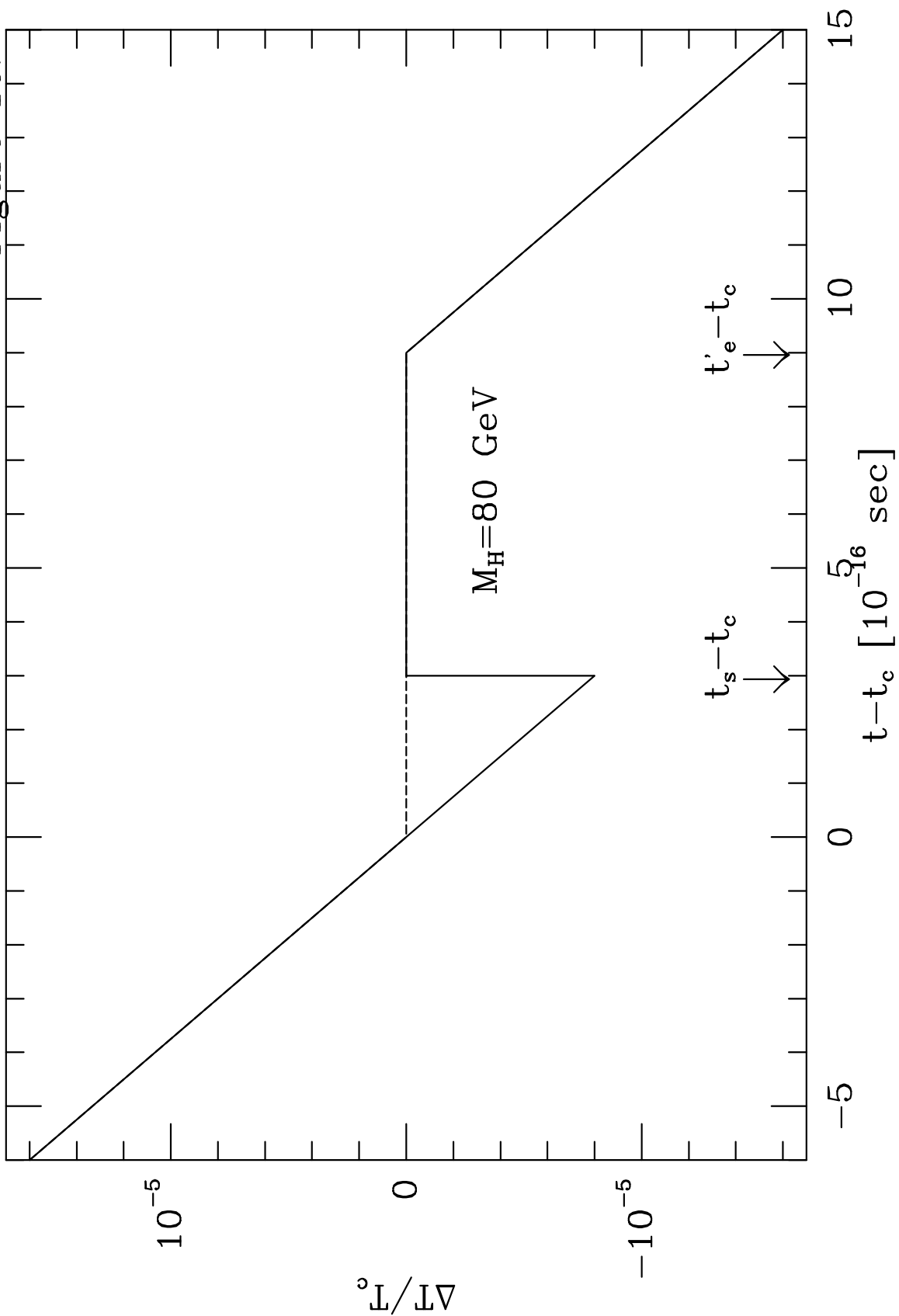


Figure 11.

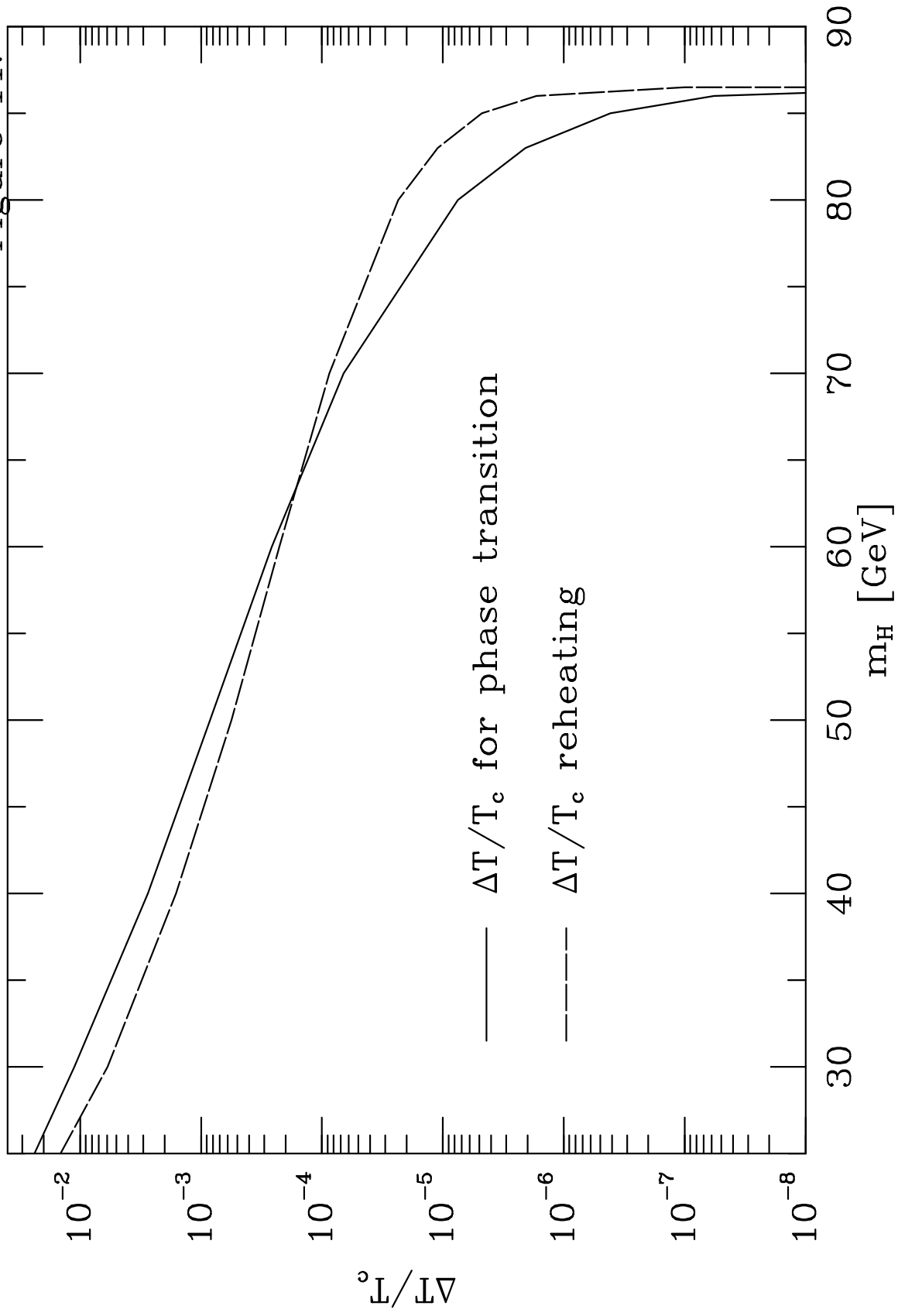


Figure 12.

